

Supporting Information for

Graded Porous Inorganic Materials Derived from  
Self-assembled Block Copolymer Templates

Yibei Gu<sup>†</sup>, Jörg G. Werner<sup>‡</sup>, Rachel M. Dorin<sup>†</sup>, Spencer W. Robbins<sup>‡</sup>, Ulrich Wiesner<sup>\*†</sup>

<sup>†</sup> Department of Materials Science and Engineering, <sup>‡</sup> Department of Chemistry and Chemical Biology,

Cornell University, Ithaca, New York 14853, United States

<sup>\*</sup>To whom correspondence should be addressed. E-mail address: [ubw1@cornell.edu](mailto:ubw1@cornell.edu)

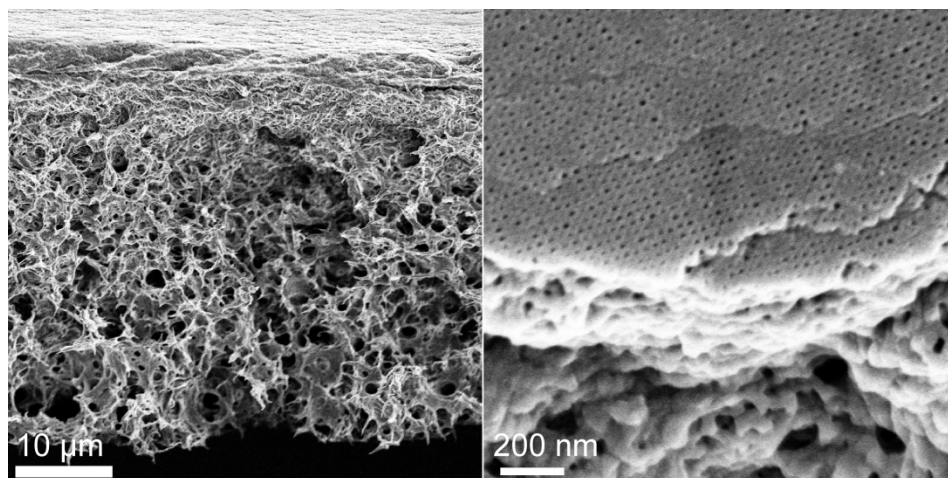


**Figure S1.** SEM images of the ISV99-35 template. The sample was sputter-coated with Au-Pd before imaging. Left: Cross-sectional image of the entire sample shows the asymmetry of the membrane. Right: Image at higher magnification of the top surface. The surface pore square lattice of the templates is clearly seen in this image, consistent with prior reports of ISV triblock terpolymer derived membranes (see Ref 25, 28 and 35 of the paper).

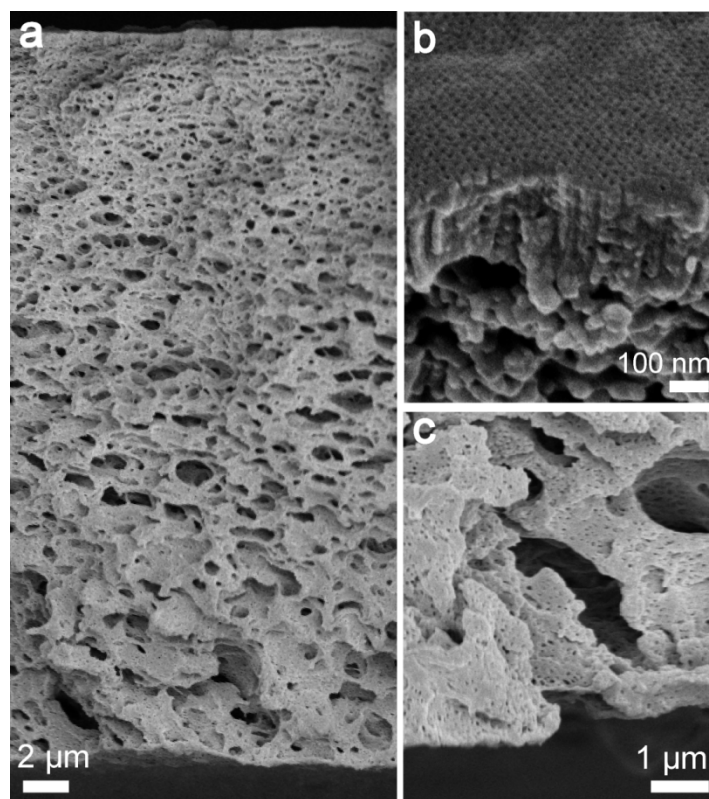


**Figure S2.** SEM images of the ISV91-33 template. The sample was sputter-coated with Au-Pd before imaging. (a) Cross-sectional image of the entire sample shows the asymmetry of the membrane. (b) Image at higher magnification of the top surface. The vertically aligned cylindrical pores are densely packed. (c) Bottom surface at a higher magnification showing both the accessible mesopores and macropores. The mesoporous template polymer strut (wall) thickness derived from these and other SEM images is  $\sim 25$  nm, consistent with previous reports on similar ISV membranes (e.g. see Ref. 35 of the paper).

### Collapse of the graded hierarchical structure:

To demonstrate the importance of the curing temperature of the phenol-formaldehyde resoles on the structural integrity of the template, Supplementary Figure S3 shows SEM images of a collapsed macrostructure after carbonization. After adsorption of the resoles from ethanolic solution to the template walls, the hybrid was cured (cross-linked) at 125 °C for 18 hours. Subsequently, for carbonization and template removal, the cross-linked hybrid materials were heated at 1 °C/min to 600 °C under N<sub>2</sub> atmosphere for 3 hours and carbonized at 1100 °C at a rate of 5 °C/min for 6 hours. Supplementary Figure S3a shows the full cross-section of the resulting carbon film with a thickness of approximately 20 μm and no remaining macroporosity. The cross-sections of the two surfaces of the film are shown with higher magnification SEM images in Supplementary Figure S3b and S3c, demonstrating that the hierarchical structure is completely lost and only mesoporosity is retained.

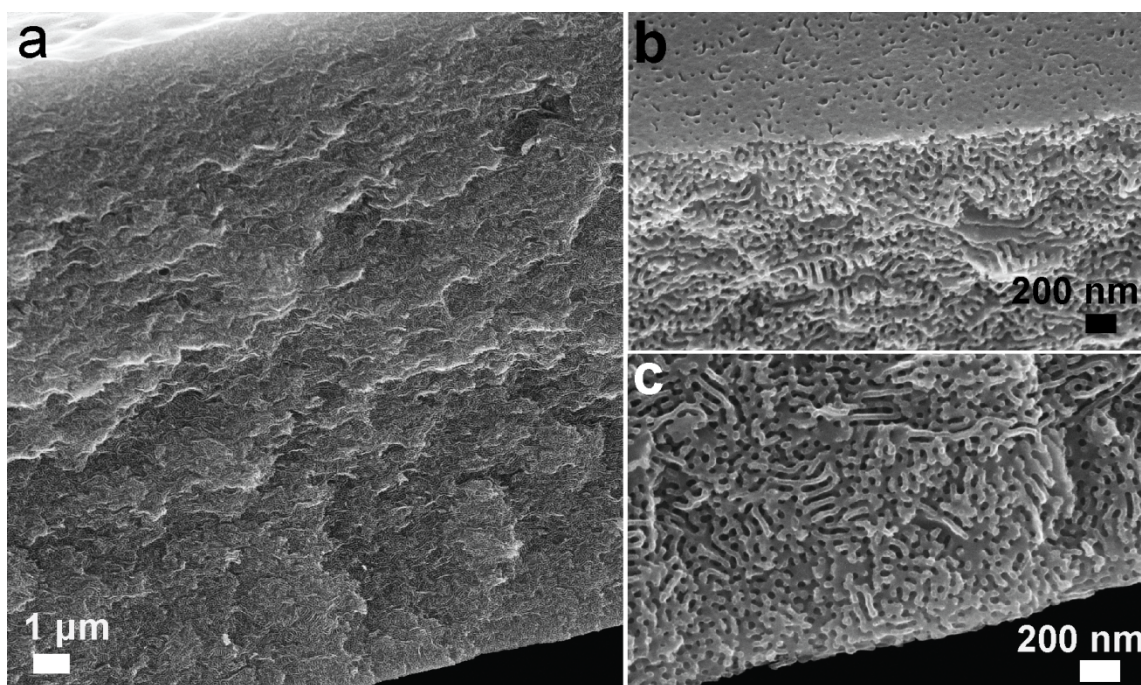


**Figure S3.** Cross-sectional SEM images of a graded carbon material (CGM-C) that was the result of a graded template film immersed in resoles solution, cured at 125 °C and carbonized at 1100 °C showing the complete loss of macroporosity and collapse of the hierarchical structure after carbonization. (a) Full cross-section of the carbon film; cross-section of the (b) top and (c) bottom surfaces of the carbonized film at higher magnification showing only mesoporosity.

### **Resorcinol-formaldehyde resoles as carbon precursor for CGM-C:**

In order to investigate the influence of the reactivity towards cross-linking of the carbon precursor, we performed the same procedure towards the formation of CGM-C as described in the main text, but using resorcinol-formaldehyde resoles. Oligomeric resorcinol-formaldehyde resoles were synthesized first. Briefly, a 50 wt% resorcinol solution in water was used and a 20 wt% sodium hydroxide solution and formalin solution were added subsequently and slowly at room temperature. The molar ratio of resorcinol:NaOH:formaldehyde was 1:0.1:1. The mixture was stirred for 10 mins at room temperature and promptly neutralized with para-toluene sulfonic acid. The red solution was freeze-dried overnight on a vacuum line and the solid resorcinol-formaldehyde resoles were dissolved in tetrahydrofuran. The resulting cloudy solution was filtered through a PTFE syringe filter (0.2 - 0.4  $\mu\text{m}$ ) to remove the precipitated sodium para-toluene sulfonate and higher molar mass resins, dried again overnight on a vacuum line and dissolved in ethanol as a 20 wt% solution. Resorcinol has an additional aromatic hydroxyl group and is therefore more reactive towards electrophilic aromatic substitution and cross-linking, even at lower temperatures than phenol-formaldehyde resoles.

Hybrids obtained from the same ISV99-35 described in the main text and resorcinol-formaldehyde resoles were cured at 90 °C for 5 days and carbonized at 1100 °C. The resulting carbon films exhibited a remarkable retention of the graded macroporous substructure, demonstrating the improved mechanical stability during the synthesis process coming from the resorcinol-formaldehyde resoles (Supplementary Figure S4a). However, the top surfaces exhibited only partially open capping layer on top of the ordered, vertically aligned carbon pillars, which most likely originated from an over-deposition of resoles on the porous skin layer of the polymer templates (Supplementary Figure S4b). Additionally, the porous walls of the macroporous substructures showed a continuous capping layer (Supplementary Figure S4c) and the bottom surfaces of the CGM-C were mostly closed off (Supplementary Figure S4d).

These results suggested that the carbon precursor must be reactive enough to cure at moderate temperatures to prevent structural collapse of the template (Supplementary Figure S3), but at the same time should not be cross-linking too fast to avoid over growth and capping layers that render the pores inaccessible.



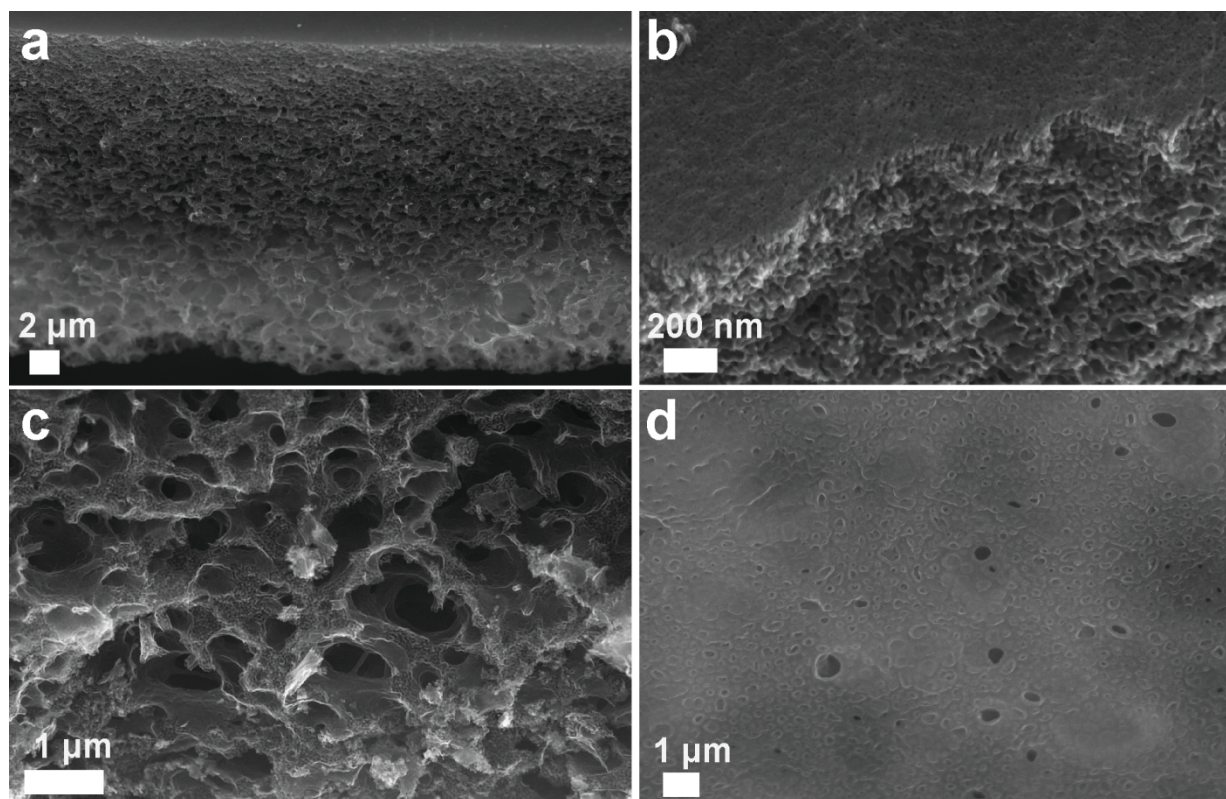


**Figure S4.** SEM images of CGM-C that was immersed in resorcinol-formaldehyde resoles and cured at 90 °C after carbonization and template removal. (a) Full cross-section demonstrating the remarkable retention of macrostructure after heat-processing using resorcinol-formaldehyde resoles as the carbon precursor. (b) Cross-section at the top surface of the CGM-C showing the formation of an only partially porous over-layer. (c) Cross-section of the macroporous bottom part of the film indicating the mesoporosity of the wall interior with capping layers towards the macropores. (d) Mostly closed off bottom surface.

# **Schematic representation of the preparation of CGM-Ni and CGM-NiO *via* Ni electroless plating:**

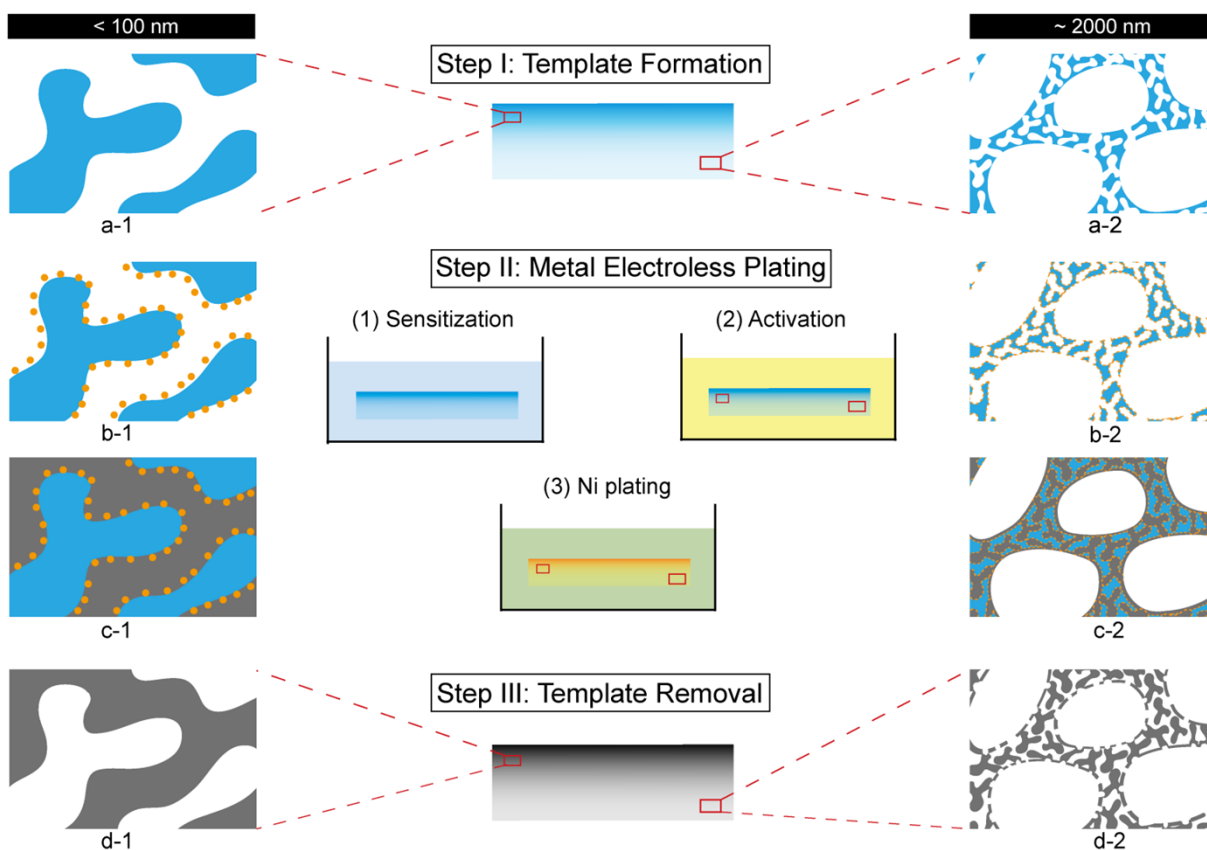


**Figure S5.** Step I: Free-standing graded hierarchically porous BCP templates are formed in water via the SNIPS process. Step II: Ni-polymer hybrids are fabricated *via* electroless plating divided into three processing steps: (1) Sensitization with  $\text{Sn}^{2+}$  complexes onto the pore surface. (2) Activation with Pd particles which serve as catalyst for the next process. (3) Ni electroless plating. In the presence of reducing agents and catalysts, Ni growth is initiated within the pores. Step III: CGM-Ni and CGM-NiO are formed after template removal by heat treatments in  $\text{N}_2$  or air, respectively. Left four figures (from a-1 to d-1) show enlarged upper portions (with mainly mesopores) of the film after each major step. Blue color represents polymer and white represents void space. The porous polymeric template (a-1) is formed. After sensitization and activation, Pd particles form onto the wall of the template (b-1, orange color represents Pd particles). After a certain plating time, the mesopores are mostly filled by Ni (c-1, grey color represents Ni). During pyrolysis in  $\text{N}_2$ , the polymeric template is removed, leaving behind the mesoporous Ni structure (d-1) (calcination in air leads to the corresponding mesoporous NiO). Right four figures (from a-2 to d-2) show enlarged lower portions of the film after each major step, where there are two length scales of pores: mesoporous sub-structures form the “walls” which connect neighboring macropores (a-2). The size difference between the mesoporous and macroporous structural features determines the extent of hierarchy. Pd particles form on the wall surfaces of the template (b-2) after sensitization and activation. The mesopores are mostly filled, while macropores are partially coated with Ni (c-2) after plating. The mesoporous voids derive from the polymer template removal while the macropores remain (d-2).

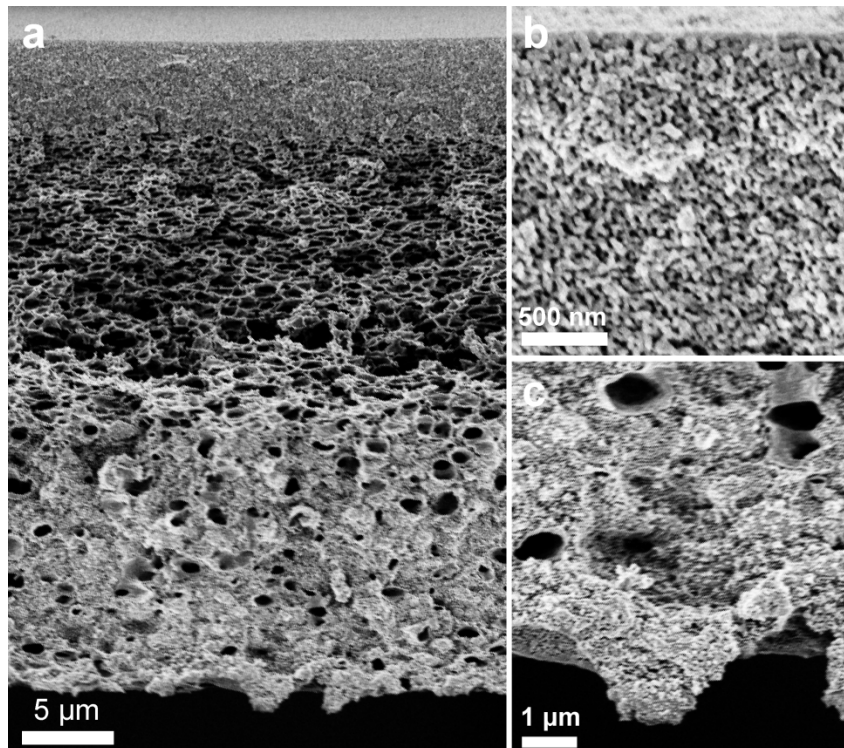


**Figure S6.** SEM images of a representative Ni-polymer hybrid film for which the rate of Ni-plating was too high, after plasma etching to remove the exposed polymer. (a) Full cross-section. Images at higher magnification near the (b) top surface and (c) bottom surface.



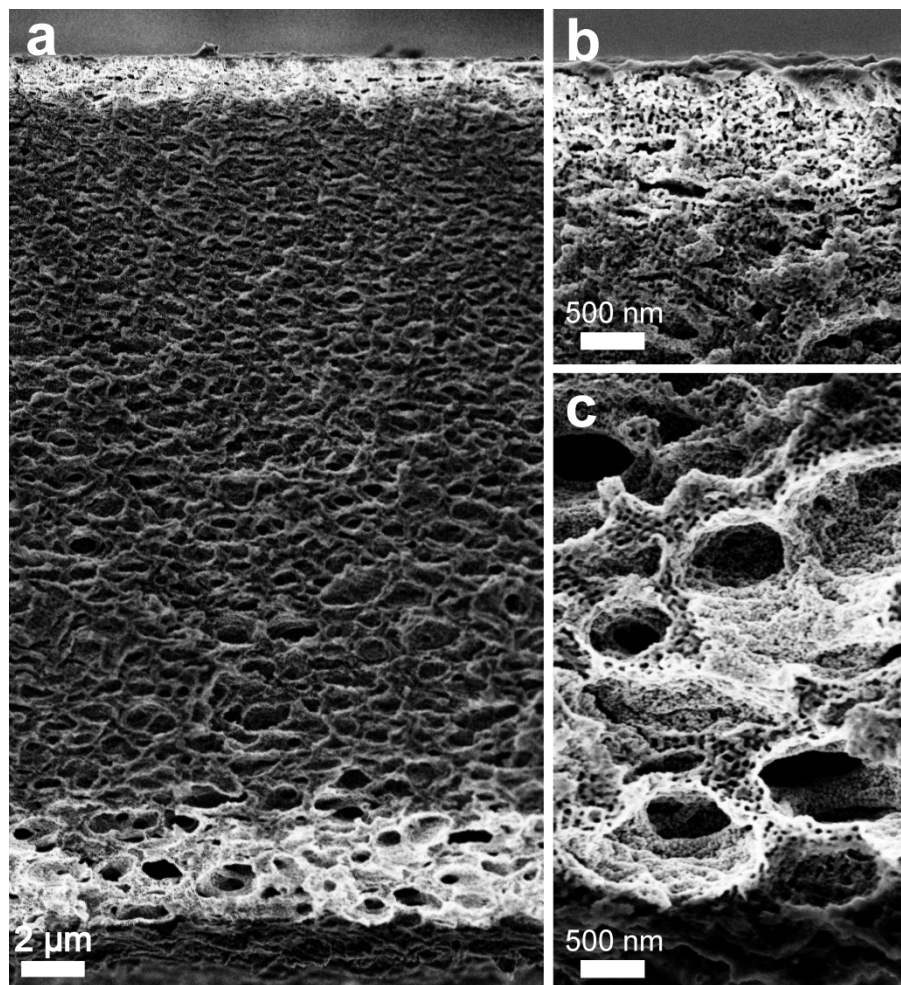


**Figure S7.** Cross-sectional SEM images of 24 h plated Ni-polymer hybrid after plasma etching for 40 min to remove the exposed polymer revealing heterogeneities in metal deposition. (a) Full cross-section. Images at higher magnification near the (b) top surface and (c) bottom surface.

## Porosity analysis

Figure 3g shows results of nitrogen sorption/desorption measurements for a representative graded porous nickel sample together with BJH pore size distribution analysis as shown in the inset. The CGM-Ni showed a large total pore volume (excluding macropores with size above 200 nm) of  $0.46 \text{ cm}^3 \text{ g}^{-1}$ , which corresponds to a high porosity of approximately 77 vol%, calculated using a nickel:palladium:carbon composition of 85:9:6 (see Table S1) and respective densities of 8.9, 12.0, and  $2.0 \text{ g/cm}^3$ , respectively. It is important to note that this porosity does not take into account macropores with a size over 200 nm. As a result, the true total porosity is even larger.

## Detailed TGA analyses

The retained sample mass under air and  $\text{N}_2$  from TGA with a heating rate of  $1^\circ\text{C/min}$  to  $600^\circ\text{C}$  from Pd-polymer hybrid films (after step II-2 in Supplementary Figure S5 and before Ni plating) was 9.3% and 14.3%, respectively.

For simplicity, in the calculations we assumed: (i) the templates carry same weight ratio of Pd catalysts after activation step; (ii) no deposits other than Ni; (iii) full oxidation of the polymer via calcination, and oxidation of Pd to PdO

$$\rightarrow \text{Weight ratio of Pd : Polymer} = \frac{M_{Pd}}{M_{PdO}} \times 9.3 : (100 - 9.3) = 8.1 : 90.7 = 0.0893$$

$$\rightarrow \text{Weight ratio of Pd : Pd-Polymer hybrids} = 8.1 : (8.1 + 90.7) = 8.2 : 100$$

Polymer is carbonized to carbon if calcined in  $\text{N}_2$ , while Pd will stay in its metallic form. So the remaining mass left from  $\text{N}_2$  calcination should be the carbon mass + Pd (14.3%)

$$\rightarrow \text{Weight ratio of Carbon : Pd-Polymer hybrids} = (14.3 - 8.2) : 100 = 6.1 : 100$$

$$\rightarrow \text{Polymer carbonization weight ratio} = \frac{6.1}{(100 - 8.2)} = 0.0664$$

$$\rightarrow \text{Polymer carbonization weight loss ratio} = 1 - 0.0664 = 0.9336$$



**Table S1. TGA calculation sheet from N<sub>2</sub> treatment**

time	Retained Weight (%) from TGA in N <sub>2</sub>	Weight Loss (%), due to polymer carbonization	Polymer wt %	Pd wt%	Ni wt%	Ni / polymer Mass Ratio
	shown in Figure 5c	= 100 – Retained Weight	= Weight Loss / 0.9336	= polymer wt% × 0.0893	= 100 – polymer wt% – Pd wt%	Ni wt% / polymer wt%
4 h	26.5	73.5	78.7	7.0	14.2	0.18
8 h	52.3	47.7	51.1	4.6	44.3	0.87
12 h	66.8	33.2	35.6	3.2	61.3	1.72

The above data is consistent with the TGA in air assuming that Ni and Pd will transform into NiO and PdO respectively, after calcination in air, while the polymer gets completely calcined away. The expected retained weight (from calculations) is compared with the actual retained weight from TGA in air in Table S2.

**Table S2. TGA calculation sheet**

time	Pd wt%	Ni wt%	PdO wt%	NiO wt%	Calculated Retained Weight (%) in air	Actual Retained Weight(%) from TGA in air
	Calculated in Table S1	Calculated in Table S1	= Pd wt% × $\frac{M_{PdO}}{M_{Pd}}$	= Ni wt% × $\frac{M_{NiO}}{M_{Ni}}$	= PdO wt% + NiO wt%	Shown in Figure 5d
4 h	7.0	14.2	8.1	18.1	26.2	33.6
8 h	4.6	44.3	5.2	56.3	61.6	59.9
12 h	3.2	61.3	3.7	77.8	81.5	80.3





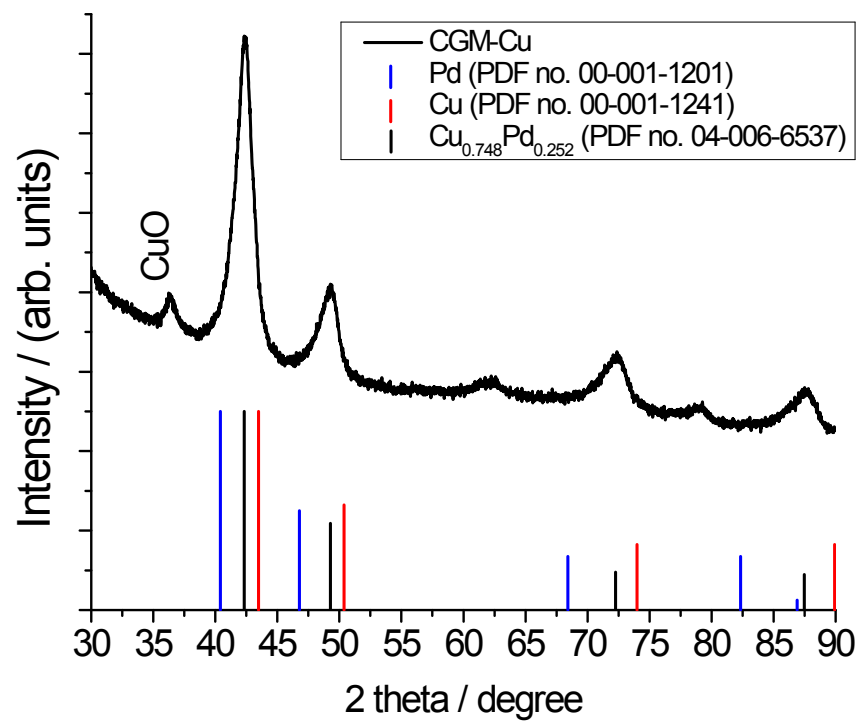


**Figure S8.** XRD pattern of CGM-Cu. The Pd and Cu formed Cu-rich alloy (Cu<sub>0.748</sub>Pd<sub>0.252</sub>), with a minor peak suggesting CuO. The crystallite size was 5 nm, approximated from the Scherrer Equation by using the main peak.